Magnetic properties of Al-Ge-Mn and Al-Cu-Ge-Mn icosahedral alloys

Z. M. Stadnik* and G. Stroink
Department of Physics, Dalhousie University, Halifax, Nova Scotia, Canada B3H 3J5
(Received 4 June 1990)

$Al_{52.5}Ge_{22.5}Mn_{25}$, $Al_{52.5}Ge_{22.5}Mn_{24.85}Fe_{0.15}$, $Al_{40}Cu_{10}Ge_{25}Mn_{25}$, and $Al_{40}Cu_{9.94}Fe_{0.06}Ge_{25}Mn_{25}$ icosahedral alloys and AlGeMn and $AlGeMn_{0.995}Fe_{0.005}$ crystalline alloys have been studied with x-ray diffraction, differential thermal analysis, magnetization, and ^{57}Fe Mössbauer spectroscopy. It is found that AlGeMn, a ferromagnet, is the major second phase present in the samples of icosahedral Al-Ge-Mn and Al-Cu-Ge-Mn systems, and is thus partially responsible for the observed ferromagnetism in these alloys. This ferromagnet is also the main crystallization product of these systems. Room-temperature ^{57}Fe Mössbauer spectra show that Fe atoms in these systems bear no magnetic moment and are distributed among a multiplicity of sites, which is interpreted as evidence of intrinsic disorder present in icosahedral alloys. Analysis of 4.2-K Mössbauer spectra shows that less than half of the Fe atoms possess a very small magnetic moment in both systems, which is the first direct evidence supporting the notion of two classes of transition-metal sites in Al-based icosahedral alloys. It is argued that the magnetic moment of Mn atoms in these systems as well as the Curie temperatures must be very small. It is noted that annealing of rapidly quenched Al-Ge-Mn and Al-Cu-Ge-Mn alloys leads to the occurrence of high values of coercive force and saturation magnetization.

I. INTRODUCTION

Icosahedral alloys studied so far exhibit diamagnetic, paramagnetic, and spin-glass properties.[1] Recently, ferromagnetism has been reported in the icosahedral $Al_{8.8}Fe_{3.7}Ce$ alloy,[2] Al-Ge-Mn and Al-Cu-Ge-Mn alloys,[3] and Si-rich Al-Mn-Si alloys.[4] The common characteristic of these alloys is a very small value of their magnetization M, which changes from a few tenths of emu/g for Al-Ge-Mn and Si-rich Al-Mn-Si alloys[3,4] to a few emu/g for $Al_{8.8}Fe_{3.7}Ce$ and Al-Cu-Ge-Mn alloys.[2,3] The reported Curie temperatures T_c are 533 K for $Al_{52.5}Ge_{22.5}Mn_{25}$,[3] 467 K for $Al_{40}Cu_{10}Ge_{25}Mn_{25}$,[3] and around 110 K for Si-rich Al-Mn-Si alloys.[4]

^{57}Fe Mössbauer-effect (ME) spectra of the icosahedral $Al_{40}Cu_{10-x}Fe_xGe_{25}Mn_{25}$ series[5-7] were interpreted in terms of a distribution of a hyperfine magnetic field. As we briefly indicated elsewhere,[8] and as will be discussed in detail in this paper, the analysis of ^{57}Fe ME spectra conducted in Refs. 5–7 is incorrect.

The surprisingly small values of M suggest the possibility that the weak ferromagnetism of these alloys may arise from a small amount of ferromagnetic second phase (or phases) present in the samples studied. This is not incompatible with x-ray diffraction spectra, since the amount of magnetic second phase required to explain the small values of M may be below the resolution of detection by an ordinary low-resolution x-ray diffraction technique. The low-resolution x-ray diffraction spectra of icosahedral alloys are not, contrary to the claims made,[2-7] single phase: Either the icosahedral lines [see, for example, the (110000) line in Fig. 2 in Ref. 3] have a visible structure or there are many low-intensity peaks which are not due to the icosahedral structure and which are usually ignored (see, for example, Fig. 1 in Ref. 4 and Fig. 1 in Ref. 5). Furthermore, the two strongest icosahedral lines (100000) and (110000) of Al-Ge-Mn and Al-Cu-Ge-Mn alloys,[3,5,6] as opposed to the corresponding lines of, for example, the $Al_{65}Cu_{20}Fe_{15}$ alloy,[9,10] are located on a rounded maximum centered at $2\theta \approx 43°$ (for Cu $K\alpha$ radiation). Since the strongest diffraction lines of various crystalline alloys also occur around this value of 2θ, the occurrence of the rounded maximum indicates the presence of some impurity in the icosahedral samples. Thus the second phase (phases) is present in a small quantity in the discussed icosahedral alloys, and if magnetic, it can account, at least partially, for their weakly ferromagnetic behavior. A careful analysis of x-ray diffraction spectra is therefore required.

A strong argument for the presence of a magnetic second phase in Si-rich Al-Mn-Si, Al-Ge-Mn, and Al-Cu-Ge-Mn icosahedral alloys is based on the comparison of their values of T_C with the T_C values of the corresponding crystalline alloys expected to be present in these icosahedral alloys as the second phases. The value of T_C observed in Si-rich, *melt-spun* amorphous Al-Mn-Si alloys of various compositions is around 110 K.[4,11-14] However, ferromagnetism almost disappears in a *sputtered* amorphous $Al_{36}Mn_{24}Si_{40}$ film.[11] In order to explain the source of the ferromagnetism in Si-rich Al-Mn-Si amorphous ribbons, and its lack in an amorphous film, Hauser *et al.*[12] studied magnetic properties of various crystalline and amorphous Si-rich Al-Mn-Si systems. They showed in an elegant way that ferromagnetism also exists in a Si-rich *crystalline* phase which was identified with β-Al-Mn-Si,[15] and which was magnetic with $T_C \approx 110$ K. Combining this important finding with the fact that ferromagnetism almost disappears in an amor-

phous $Al_{36}Mn_{24}Si_{40}$ film, Hauser *et al.*[12] concluded that the ferromagnetism observed in Si-rich Al-Mn-Si amorphous ribbons of various compositions may be an extrinsic effect; i.e., it may arise from a small amount of Al-Mn-Si microcrystallinity with $T_c \approx 110$ K. As mentioned earlier, the values of T_c of Si-rich icosahedral Al-Mn-Si alloys are also around 110 K.[4,7,14] It would be very unusual for all Si-rich Al-Mn-Si alloys of different compositions and structure (amorphous, icosahedral, and crystalline) to have practically the same value of T_C around 110 K. The clue to this unusual behavior lies in the work of Hauser *et al.*,[12] which was not referred to in the reports claiming ferromagnetism in Si-rich amorphous and icosahedral alloys.[4,7,13,14] Namely, the ferromagnetism in Si-rich Al-Mn-Si amorphous ribbons and icosahedral alloys may be not an intrinsic property of these materials, but is most probably due to a small amount of magnetic Al-Mn-Si microcrystallinity with $T_C \approx 110$ K. In view of this, the description in recent review articles,[16,17] which do not refer to the crucial work of Hauser *et al.*,[12] of the apparent ferromagnetism of Si-rich Al-Mn-Si icosahedral alloys as a well-established fact seems to be premature.

The reported T_C value of 533 K for $Al_{52.5}Ge_{22.5}Mn_{25}$ (Ref. 3) is in good agreement with the value of 529(5) K determined by us.[8] The latter value was also found for icosahedral $Al_{55.5}Ge_{21}Mn_{23.5}$ and $Al_{57.5}Ge_{20}Mn_{22.5}$ alloys.[18] The T_C value of 467 K for $Al_{40}Cu_{10}Ge_{25}Mn_{25}$ is lower than the value of 528(10) K determined by us.[18] The above values of T_C are very close to $T_C = 519$ K of a crystalline ferromagnet AlGeMn whose saturation magnetization is about 62 emu/g.[19] This indicates that the AlGeMn crystalline phase may be present in Al-Ge-Mn and Al-Cu-Ge-Mn icosahedral alloys, and it may be partially responsible for the observed ferromagnetism of these alloys. More detailed studies, using x-ray diffraction, transmission electron microscopy, and other magnetic probes, of these alloys are necessary to elucidate the source of their apparent ferromagnetism.

Another indication of the presence of a magnetic second phase in Al-Ge-Mn and Al-Cu-Ge-Mn icosahedral alloys is based on comparing their values of M with the values of the coercive force H_c, which is about 2 kOe.[3,8,18] One would hardly expect such a value of H_c and a minute value of M for a homogeneous magnet with a high value of T_C.

The ME technique has proved to be very useful in studies of magnetism of various materials. Unfortunately, because of methodological errors, which are discussed in this paper, in the analysis of complex ^{57}Fe ME spectra, previous ^{57}Fe ME studies[5,6] of the $Al_{40}Cu_{10-x}Ge_{25}Mn_{25}$ series contributed to the confusion in the field of magnetism of icosahedral alloys.

The purpose of this paper is to elucidate the source of the observed ferromagnetism in Al-Ge-Mn and Al-Cu-Ge-Mn icosahedral alloys. We combine x-ray diffraction, differential thermal analysis, ^{57}Fe ME, and magnetization techniques to study these alloys and also a crystalline Al-GeMn alloy. To perform ^{57}Fe measurements on these systems, an impurity concentration of Fe enriched in a ^{57}Fe isotope was introduced to the alloys.

II. EXPERIMENT

Ingots of composition $Al_{52.5}Ge_{22.5}Mn_{25}$, $Al_{52.5}Ge_{22.5}Mn_{24.85}Fe_{0.15}$, $Al_{40}Cu_{10}Ge_{25}Mn_{25}$, $Al_{40}Cu_{9.94}Fe_{0.06}Ge_{25}Mn_{25}$, AlGeMn, and $AlGeMn_{0.995}Fe_{0.005}$ were prepared by arc melting in an argon atmosphere of high-purity elemental constituents. The iron metal used was enriched to 95% in the ^{57}Fe isotope. The ingots corresponding to icosahedral compositions were melt spun in air by ejecting molten alloy at a temperature estimated with a pyrometer to be in the range 1373–1423 K through a 0.7-mm-diam orifice in a quartz tube onto the surface of a rotating copper wheel 15 cm in diameter. The tangential velocity of the wheel was 70(1) m/s, and the ejection pressure of argon was about 55 kPa. The resulting alloys were in the form of brittle flakes. The AlGeMn and $AlGeMn_{0.995}Fe_{0.005}$ ingots were vacuum annealed at 973 K for 24 h.

Room-temperature x-ray diffraction (XRD) measurements were performed on a Siemens D500 scanning diffractometer using Cu $K\alpha$ radiation. The contribution to the spectra from the Cu $K\alpha_2$ radiation was subtracted. X-ray scans were carried out with a 2θ step of 0.05° and a time per step of 5 s. The alloys were gently powdered for x-ray measurements.

^{57}Fe ME measurements were performed at room temperature and 4.2 K using a Wissel MSII Mössbauer spectrometer operating in a sine or triangular mode. The spectrometer was calibrated with a 12.7-μm-thick Fe foil,[20] and the spectra were folded. The surface densities of the $Al_{52.5}Ge_{22.5}Mn_{24.85}Fe_{0.15}$, $Al_{40}Cu_{9.94}Fe_{0.06}Ge_{25}Mn_{25}$, and $AlGeMn_{0.995}Fe_{0.005}$ Mössbauer absorbers were respectively 12.6×10^{-3}, 4.0×10^{-3}, and 47.6×10^{-3} mg ^{57}Fe/cm^2. The source used was ^{57}Co(Rh).

Magnetization measurements at room temperature were conducted in fields up to 9 kOe using a vibrating-sample magnetometer.

Differential thermal analysis (DTA) measurements were carried out under an argon atmosphere on a Fisher 260F thermal analyzer using a heating rate of 20 K min^{-1}.

III. RESULTS AND DISCUSSION

A. Differential thermal analysis and x-ray diffraction data

A DTA curve of an $Al_{52}Ge_{22.5}Mn_{24.85}Fe_{0.15}$ icosahedral alloy exhibits an exothermic peak resulting from the transformation of icosahedral to equilibrium crystalline phases at temperatures ranging from the onset for the crystallization temperature T_x, 719 K, to 745 K. For an $Al_{40}Cu_{9.94}Fe_{0.06}Ge_{25}Mn_{25}$ icosahedral alloy, the corresponding temperature range is 592–643 K. These values of T_x are in reasonably good agreement with the values of 685 K for $Al_{52.5}Ge_{22.5}Mn_{25}$ and 608 K for $Al_{40}Cu_{10}Ge_{25}Mn_{25}$ icosahedral alloys reported by Tsai *et al.*[3] for a heating rate of 40 K min^{-1} and unspecified quenching rate parameters.

The XRD patterns of crystalline AlGeMn and $AlGeMn_{0.995}Fe_{0.005}$ are shown in Figs. 1(a) and 1(b). All lines present in the patterns could be indexed on the basis of a tetragonal cell, in agreement with previous structural studies of the AlGeMn alloy.[21] The values of lattice constants, a and c, obtained from least-squares fits of the observed XRD line positions are 3.926(2) and 5.962(3) Å for AlGeMn, and 3.919(1) and 5.946(2) Å for $AlGeMn_{0.995}Fe_{0.005}$. The smaller values of a and c for $AlGeMn_{0.995}Fe_{0.005}$ than for AlGeMn are in accordance

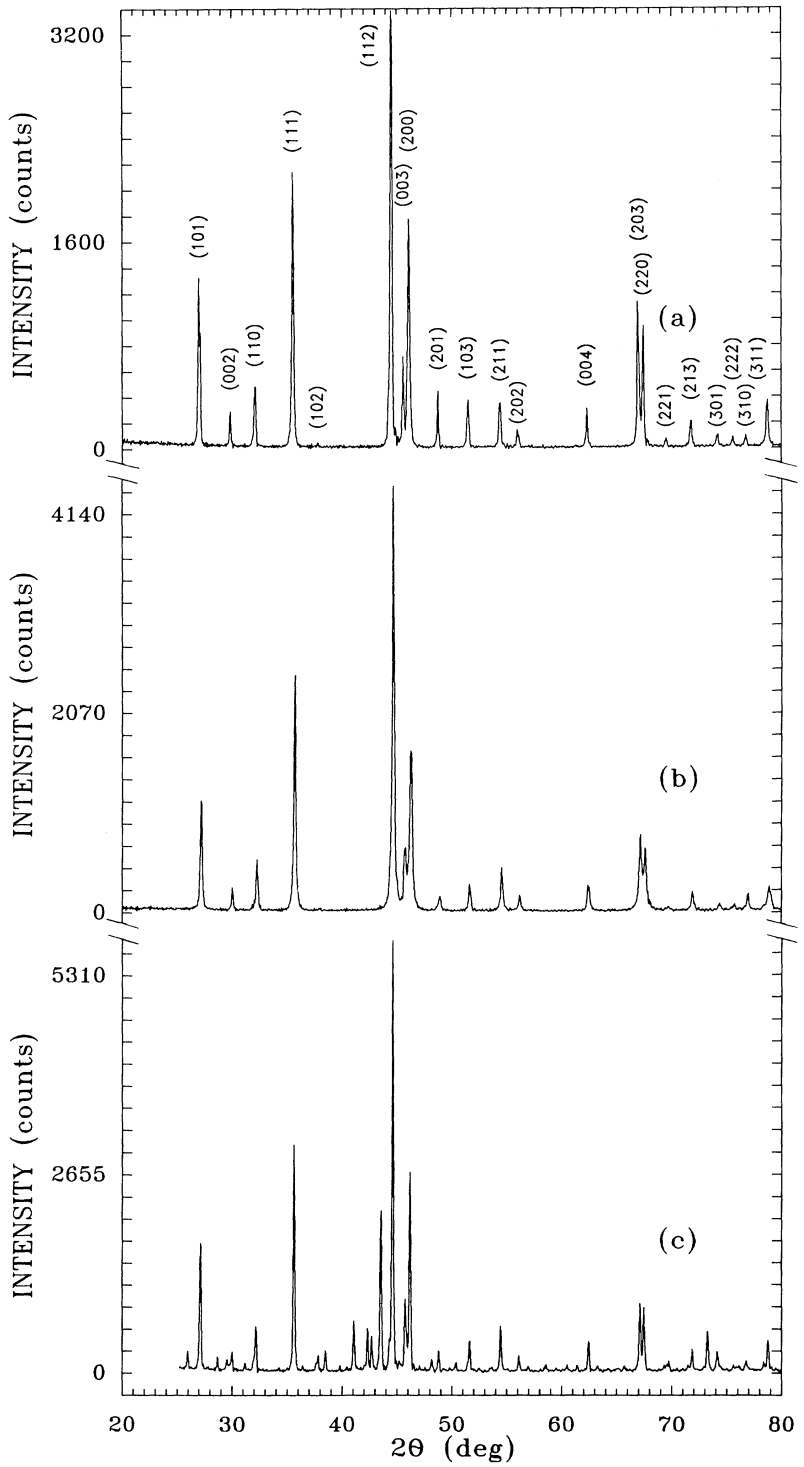

FIG. 1. X-ray-diffraction patterns obtained with Cu $K\alpha_1$ radiation of (a) crystalline AlGeMn, (b) crystalline $AlGeMn_{0.995}Fe_{0.005}$, and (c) icosahedral $Al_{52.5}Ge_{22.5}Mn_{24.85}Fe_{0.15}$ heated up to 799 K at a rate of 20 K min^{-1} in a DTA analyzer.

with what can be expected on the basis of the atomic radii of Mn and Fe.

A comparison between the XRD pattern of crystallized $Al_{52.5}Ge_{22.5}Mn_{24.85}Fe_{0.15}$ [Fig. 1(c)] and the pattern of AlGeMn [(Fig. 1(a)] clearly shows that the main crystallization product of icosahedral $Al_{52.5}Ge_{22.5}Mn_{24.85}Fe_{0.15}$ is the AlGeMn alloy. Other minor peaks in Fig. 1(c) could not be assigned unambiguously to a specific alloy. They are most probably due to some compositions of the binary Mn-Ge system in which various magnetic alloys are known to be formed.[22] The XRD pattern of crystallized $Al_{40}Cu_{9.94}Fe_{0.06}Ge_{25}Mn_{25}$ [Fig. 2(b)] is very similar to that in Fig. 1(c). We thus conclude that the main crystallization product of Al-Ge-Mn and Al-Cu-Ge-Mn icosahedral alloys is a tetragonal AlGeMn alloy.

The XRD pattern of icosahedral $Al_{40}Cu_{9.94}Fe_{0.06}Ge_{25}Mn_{25}$ shown in Fig. 2(a) is similar to the patterns observed earlier[5,6] for icosahedral $Al_{40}Cu_{10}Ge_{25}Mn_{25}$ and $Al_{40}Cu_7Fe_3Ge_{25}Mn_{25}$ [the line with the indices (110001) at $2\theta \approx 27°$ in Refs. 5 and 6 should have the indices $(11\bar{1}0\bar{1}0)$]. The indexing of the icosahedral XRD lines in Figs. 2(a) and 3(a) is according to the scheme of Bancel *et al.*[23] The "quasilattice constant" a_R (the edge length of the rhombic dodecahedron cells that make up the three-dimensional Penrose tiling[24,25]) was calculated from the formula $13.308/Q(100000)$,[25] where $Q(100000)$ is the scattering wave vector ($Q = 4\pi \sin\theta/\lambda$) corresponding to the (100000) line. The values of a_R are 4.550(2) and 4.526(2) Å for $Al_{40}Cu_{10}Ge_{25}Mn_{25}$ and $Al_{40}Cu_{9.94}Fe_{0.06}Ge_{25}Mn_{25}$, respectively. The observed decrease of a_R associated with the substitution of Cu by Fe is expected on the basis of atomic radii of Cu and Fe. The positions of all icosahedral lines indicated in Fig. 2(a) [and also in Fig. 3(a)] were calculated[23] from the position of the (100000) line. The centers of the labels of the icosahedral Miller indices in Figs. 2(a) and 3(a) [except the labels (100000) and (110000)] correspond to the calculated positions of the icosahedral lines.

It is clear from Fig. 2(a) that, in addition to icosahedral lines, there are also other lines due to small amounts of second phases. The centers of the symbols * correspond (in an increasing 2θ sequence) to the positions of (101), (111), and (200) lines and to the average position of narrowly separated (203) and (220) lines of an $AlGeMn_{0.995}Fe_{0.005}$ ferromagnet from Fig. 1(b). The (101) line of AlGeMn [the first * symbol in Fig. 2(a)] strongly overlaps with the icosahedral $(11\bar{1}0\bar{1}0)$ line and therefore is not seen separately. The overlap of the (111) line [the second * symbol in Fig. 2(a)] with the $(21\bar{1}001)$ line is smaller, and the former line can be distinguished from a much weaker $(21\bar{1}001)$ line present to its right. The strongest line of AlGeMn [(112)], which is not indicated in Fig. 2(a), coincides with the (110000) icosahedral line. The most visible proof of the presence of AlGeMn as a second phase in the $Al_{40}Cu_{9.94}Fe_{0.06}Ge_{25}Mn_{25}$ icosahedral sample is the occurrence of a well-separated (200) line [the third * symbol in Fig. 2(a)] and the (203)–(220) lines [the fourth * symbol in Fig. 2(a)]. One can also clearly see the AlGeMn (200) and (203)–(220) impurity lines in the XRD patterns of an $Al_{40}Cu_{10-x}Fe_xGe_{25}Mn_{25}$ icosahedral system published in the literature.[5,6] It should be emphasized that we used different quenching rates (by changing the tangential velocity of the wheel, the diameter of the orifice, the ejection pressure, and the temperature of the molten alloy) in order to try to eliminate the presence of any AlGeMn second phase. In spite of this, it was not possible to produce $Al_{40}Cu_{10-x}Fe_xGe_{25}Mn_{25}$ icosahedral samples with less impurity than for the sample whose XRD pattern is shown in Fig. 2(a). We thus conclude that the major second phase present in an icosahedral $Al_{40}Cu_{10-x}Fe_xGe_{25}Mn_{25}$ system produced by the rapidly quenched technique is an AlGeMn ferromagnet, which must be responsible, at least partially, for the observed ferromagnetism[3] in the icosahedral $Al_{40}Cu_{10}Ge_{25}Mn_{25}$ alloy.

As mentioned in the Introduction, the two strongest icosahedral lines (100000) and (110000) are located on a rounded maximum [Fig. 2(a) and figures in Refs. 5 and 6], which must be due to the presence of overlapping lines of other second phases. The presence of other minor peaks present in Fig. 2(a) could not be associated unambiguously with a specific alloy (alloys), although the two strongest XRD lines of $Ge_{25}Mn_5$ (Ref. 26) match reasonably well with two of the three features seen between the (100000) and (110000) lines in Fig. 2(a).

The XRD patterns of $Al_{52.5}Ge_{22.5}Mn_{24.85}Fe_{0.15}$ produced in three different squirts, each with a different melt temperature, are shown in Fig. 3. The values of a_R for $Al_{52.5}Ge_{22.5}Mn_{25}$ and $Al_{52.5}Ge_{22.5}Mn_{24.85}Fe_{0.015}$ are 4.543(3) and 4.551(6) Å, respectively. Although there seems to be a slight increase of a_R with the substitution of Mn by Fe, which is contrary to what is expected on the basis of atomic radii of Mn and Fe, this increase cannot be given any significance since it lies within experimental error. Since all the lines in the XRD pattern in Fig. 3(a) can be assigned to suitable icosahedral Miller indices, a sample with such an XRD pattern could be declared a single-phase icosahedral alloy.[3] However, a closer analysis of the XRD pattern in Fig. 3(a), which corresponds to the best, i.e., with the smallest amount of second phases, $Al_{52.5}Ge_{22.5}Mn_{25-x}Fe_x$ alloy we could produce, shows that the broad $(11\bar{1}0\bar{1}0)$ line consists in fact of two strongly overlapping lines: an icosahedral $(11\bar{1}0\bar{1}0)$ line of larger intensity and a (100) line of smaller intensity due to an AlGeMn second phase. This is clearly demonstrated in Figs. 3(b) and 3(c), which are the XRD patterns of $Al_{52.5}Ge_{22.5}Mn_{24.85}Fe_{0.15}$ with progressively increasing content of the second phases. It can be seen that the intensity ratio of the $(11\bar{1}0\bar{1}0)$ line and the (100) line [the first * symbol in Fig. 3(c)] is reversed in Fig. 3(c) as compared to this ratio in Fig. 3(a). Furthermore, the (200) line due to an AlGeMn ferromagnet, which contributes to the hump at the right side of the (110000) icosahedral line in Fig. 3(a), is clearly visible in Fig. 3(c) [the third * symbol in Fig. 3(c)]. Additionally, the two strongest icosahedral lines in Fig. 3 are located on a rounded maximum, which arises from overlapping lines of other impurity phases. Similarly to the $Al_{40}Cu_{10-x}Ge_{25}Mn_{25}$ system discussed above, the two strongest XRD lines of Ge_2Mn_5 seem to contribute to the

features between the two strongest icosahedral lines in Fig. 3. However, an unambiguous determination of other than AlGeMn phases was not possible. We thus conclude that in the rapidly quenched $Al_{52.5}Ge_{22.5}Mn_{25-x}Fe_x$ icosahedral system, similarly to the $Al_{40}Cu_{10-x}Fe_xGe_{25}Mn_{25}$ icosaheral system, a small amount of a ferromagnetic AlGeMn is present as a second phase and therefore must be responsible, at least partially, for the observed ferromagnetism in this system.[3,8]

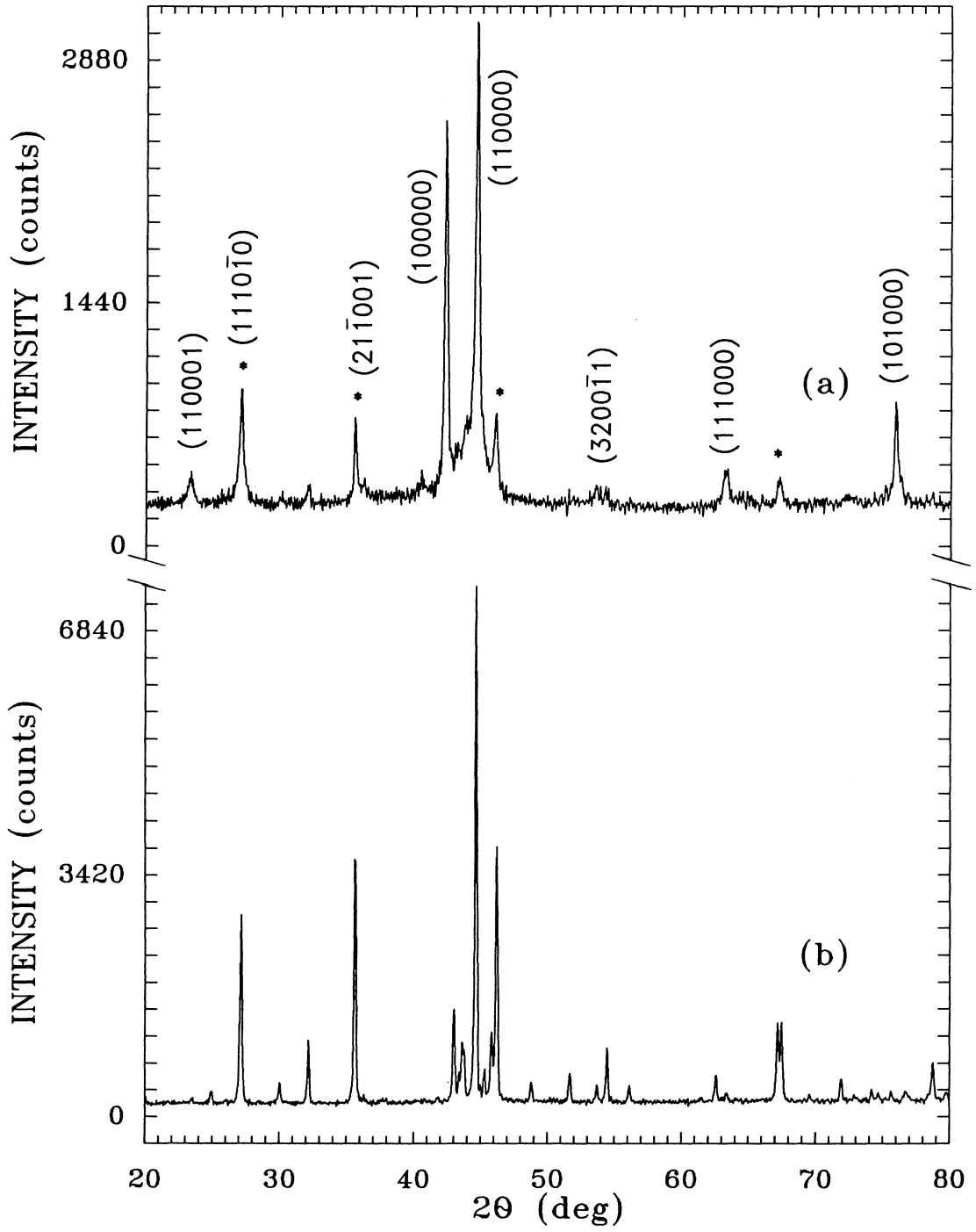

FIG. 2. X-ray-diffraction patterns obtained with Cu $K\alpha_1$ radiation of icosahedral $Al_{40}Cu_{9.94}Fe_{0.06}Ge_{25}Mn_{25}$ (a) in an as-quenched state and (b) heated up to 798 K at a rate of 20 K min^{-1} in a DTA analyzer. The centers of the symbols * in (a) correspond (in an increasing 2θ sequence) to the positions of (101), (111), and (200) lines, and the average position of narrowly separated (203) and (220) lines of $AlGeMn_{0.995}Fe_{0.005}$ from Fig. 1(b).

B. Magnetization data

The room-temperature values of magnetization measured in an applied field of 9 kOe, M_9, for the samples whose XRD patterns are shown in Figs. 3(a)–3(c) are, respectively, 0.27, 2.98, and 4.15 emu/g [Figs. 4(a)–4(c)]. The value of 0.27 emu/g is close to the value of 0.33 emu/g (Fig. 3 in Ref. 3) found earlier for $Al_{52.5}Ge_{22.5}Mn_{25}$. One can see that the measured values of M_9 correlate well with the content of AlGeMn and

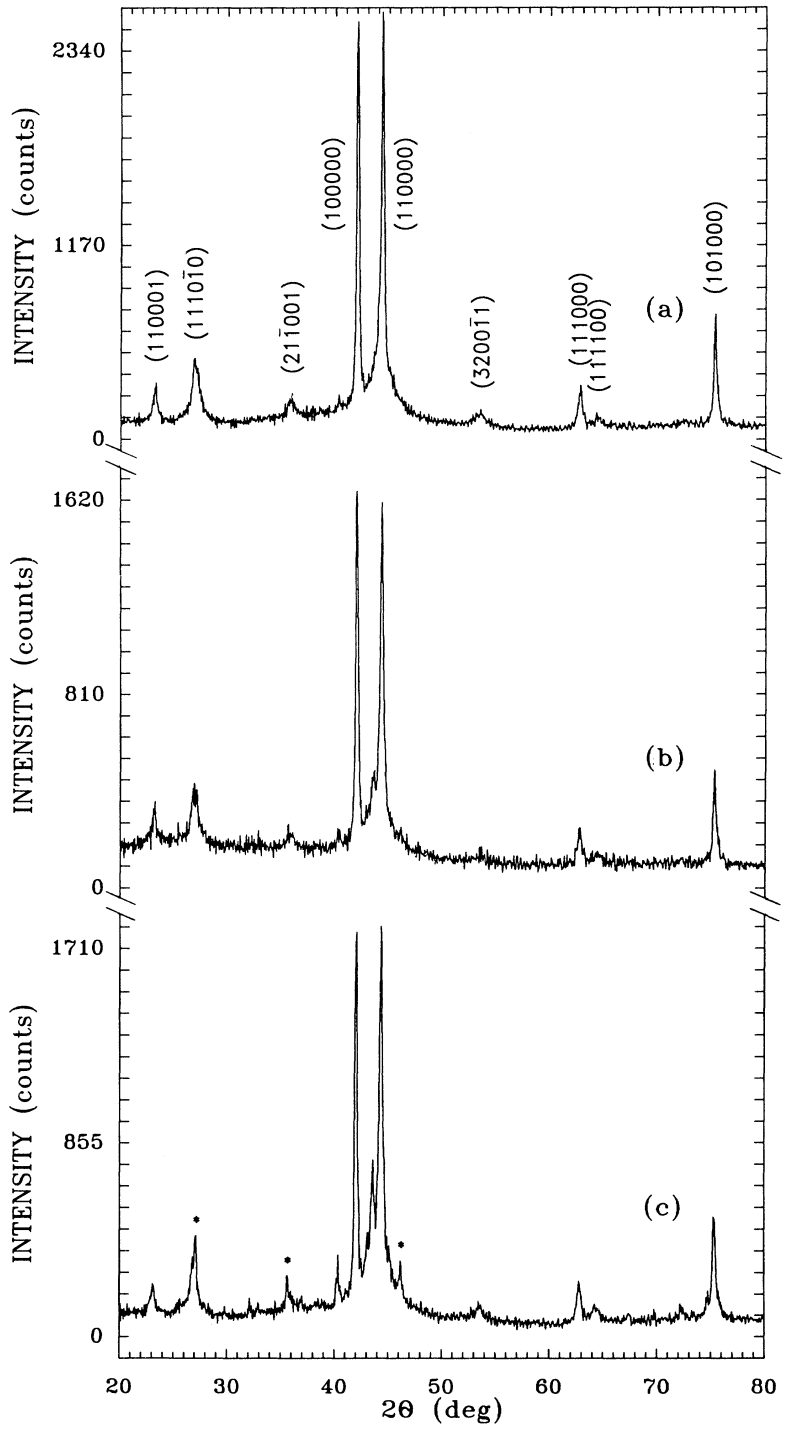

FIG. 3. X-ray-diffraction patterns obtained with Cu $K\alpha_1$ radiation of icosahedral $Al_{52.5}Ge_{22.5}Mn_{24.85}Fe_{0.15}$ produced in three separate squirts as described in the text. The centers of the symbols * in (c) correspond (in an increasing 2θ sequence) to the positions of (101), (111), and (200) lines of $AlGeMn_{0.995}Fe_{0.005}$ from Fig. 1(b).

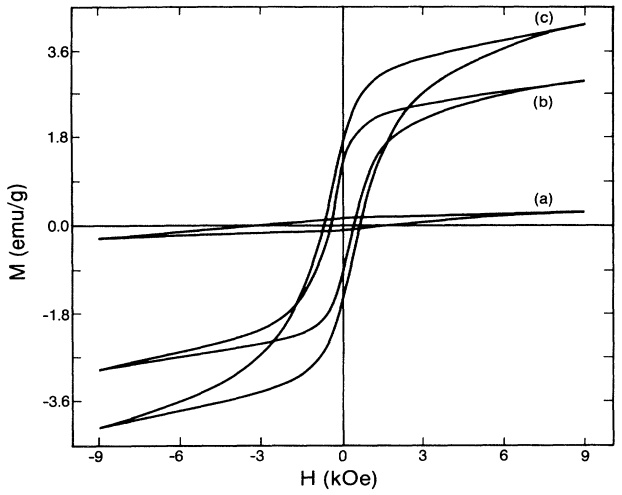

FIG. 4. Room-temperature hysteresis curves for $Al_{52.5}Ge_{22.5}Mn_{24.85}Fe_{0.15}$ icosahedral alloys whose x-ray-diffraction patterns are shown in Fig. 3.

other second phases present in the XRD patterns in Fig. 3. A similar correlation was observed for the $Al_{40}Cu_{10-x}Fe_xGe_{25}Mn_{25}$ ($x=0.0$ or 0.06) icosahedral system, for which M_9 varied in the range 2.3–30.0 emu/g, depending on the amount of AlGeMn and other second phases present. This correlation confirms the conclusion made earlier on the basis of the XRD patterns about the presence of AlGeMn and possibly other magnetic second phases in melt-spun samples of $Al_{52.5}Ge_{22.5}Mn_{25-x}Fe_x$ and $Al_{40}Cu_{10-x}Fe_xGe_{25}Mn_{25}$ icosahedral systems.

Substitution for Cu in icosahedral $Al_{40}Cu_{20}Ge_{25}Mn_{25}$ by even a very small amount of Fe leads to a noticeable decrease of M (Fig. 5). This has been also found for icosahedral $Al_{52.5}Ge_{22.5}Mn_{25-x}Fe_x$ with $x=0.0$ and

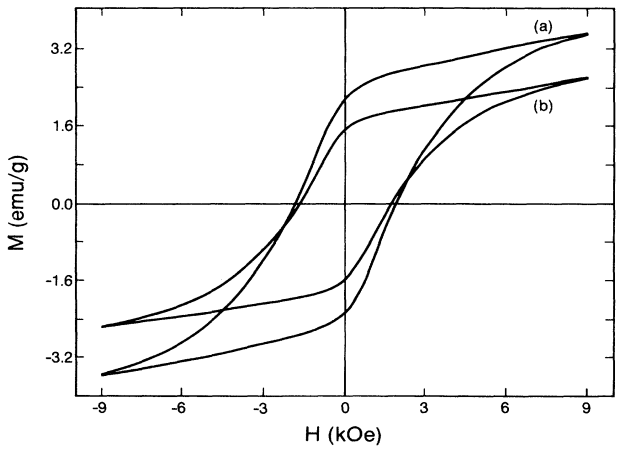

FIG. 5. Room-temperature hysteresis curves for icosahedral (a) $Al_{40}Cu_{10}Ge_{25}Mn_{25}$ and (b) $Al_{40}Cu_{9.94}Fe_{0.06}Ge_{25}Mn_{25}$.

0.15. Similar behavior was observed earlier in Mn-rich crystalline alloys.[27,28]

It was observed that after a DTA treatment these icosahedral alloys increase significantly their values of M_9 and, rather unexpectedly, also their values of H_c. For example, the values of M_9 and H_c for the crystallized sample whose XRD pattern is shown in Fig. 1(c) are, respectively, 10.3 emu/g and 3.4 kOe. The corresponding values for the crystallized sample whose XRD pattern is shown in Fig. 2(b) are 18.5 emu/g and 5.3 kOe. This suggests that melt-spun icosahedral Al-Ge-Mn and Al-Cu-Ge-Mn alloys subjected to suitable thermal processing conditions have the potential for being used as materials for producing hard magnets.

C. ^{57}Fe Mössbauer effect data

It is clear from the analysis presented above that the AlGeMn ferromagnet is the main second phase present in melt-spun Al-Ge-Mn and Al-Cu-Ge-Mn icosahedral alloys. Its presence is clearly visible in XRD patterns of the best samples of $Al_{40}Cu_{10-x}Ge_{25}Mn_{25}$ icosahedral alloys we could produce, whereas it is less visible in XRD patterns of the best samples of $Al_{52.5}Ge_{22.5}Mn_{25-x}Fe_x$ icosahedral alloys. AlGeMn must be then partially responsible for the observed ferromagnetism of these alloys. This, however, does not prove that these icosahedral alloys are not magnetically ordered. One thing seems to be evident: If they are magnetically ordered, their M values must be very small indeed (smaller than the values found in this paper for the best samples and in the literature[3,8]), and one would therefore expect that their values of T_C will be significantly smaller than those reported.[3,8] The question of whether these alloys are or are not magnetically ordered cannot be decided unambiguously by magnetization measurements alone since the contributions to M from AlGeMn impurity and from a possibly magnetically ordered icosahedral alloy cannot be separated. This question, however, can be elucidated by ^{57}Fe ME measurements because of a very favorable, although quite fortuitous, coincidence. Normally, one observes for a ferromagnet at temperatures below T_C a magnetically split ^{57}Fe ME Zeeman spectrum.[29] However, in the specific case of the AlGeMn ferromagnet, in spite of the fact that the magnetic moment of Mn at 4.2 K is $1.70\mu_B$,[19] the hyperfine magnetic field at 4.2 K at ^{57}Fe nuclei of Fe atoms substituting in impurity concentrations for Mn atoms is zero. This is demonstrated in Fig. 6, in which one can see only an asymmetric doublet due to an electric quadrupole interaction. Thus Fe atoms in impurity concentrations substituting for Mn atoms in the AlGeMn ferromagnet do not carry a magnetic moment. This fact was discovered earlier by Shinohara, Kurosawa, and Onodera[27] for the $AlGeMn_{1-x}Fe_x$ series with $x \geq 0.01$ in the temperature range 86–516 K. Consequently, in spite of the fact that AlGeMn(Fe) impurity is present in Al-Ge-Mn(Fe) and Al-Cu(Fe)-Ge-Mn icosahedral alloys, its contributions to a Mössbauer spectrum will not be in the form of a Zeeman pattern. This means that, despite the presence of the ferromagnetic AlGeMn, the occurrence of a Zeeman pattern in ^{57}Fe ME spectra of these alloys

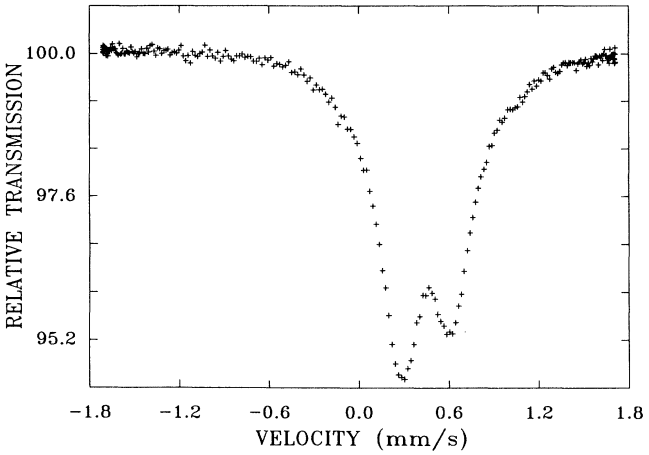

FIG. 6. ^{57}Fe Mössbauer spectrum of $AlGeMn_{0.995}Fe_{0.005}$ at 4.2 K. The velocity scale is relative to the ^{57}Co(Rh) source.

can indicate, as discussed below, that the icosahedral alloys themselves are magnetically ordered.

Room-temperature ^{57}Fe Mössbauer spectra of $Al_{52.5}Ge_{22.5}Mn_{24.85}Fe_{0.15}$ and $Al_{40}Cu_{9.94}Fe_{0.06}Ge_{25}Mn_{25}$ alloys were measured first using a large velocity range (Fig. 7) in order to detect a possible Zeeman splitting. The spectra in Fig. 7 show only an asymmetric doublet due to an electric quadrupole interaction. The lack of a Zeeman pattern proves that the hyperfine magnetic field at ^{57}Fe nuclei is zero, and consequently Fe atoms in these alloys do not carry a magnetic moment at room temperature. The corresponding spectra at 4.2 K (Fig. 8) show a hardly noticeable broadening caused by the occurrence of a very small magnetic dipole interaction for $Al_{52.5}Ge_{22.5}Mn_{24.85}Fe_{0.15}$ [Fig. 8(a)] and a small, but clearly visible broadening for $Al_{40}Cu_{9.94}Fe_{0.06}Ge_{25}Mn_{25}$ [Fig. 8(b)]. Thus the ^{57}Fe Mössbauer spectra shown in Figs. 7 and 8 prove that Fe atoms in these icosahedral alloys bear no magnetic moment at room temperature and could bear a very small magnetic moment at 4.2 K.

In order to study in detail the hyperfine interaction in these alloys, their room-temperature and 4.2-K ^{57}Fe Mössbauer spectra were remeasured using a small velocity scale. The room-temperature spectra [Figs. 9(a) and 9(b)] exhibit a quadrupole doublet structure. The full linewidth at half maximum, Γ, of two Lorentzian lines obtained from a fit with an asymetric doublet are 0.389(2) and 0.412(3) mm/s for the experimental spectrum in Fig. 9(a), and 0.395(7) and 0.433(7) mm/s for the experimental spectrum in Fig. 9(b). Such large broadening of component lines as compared to the natural linewidth

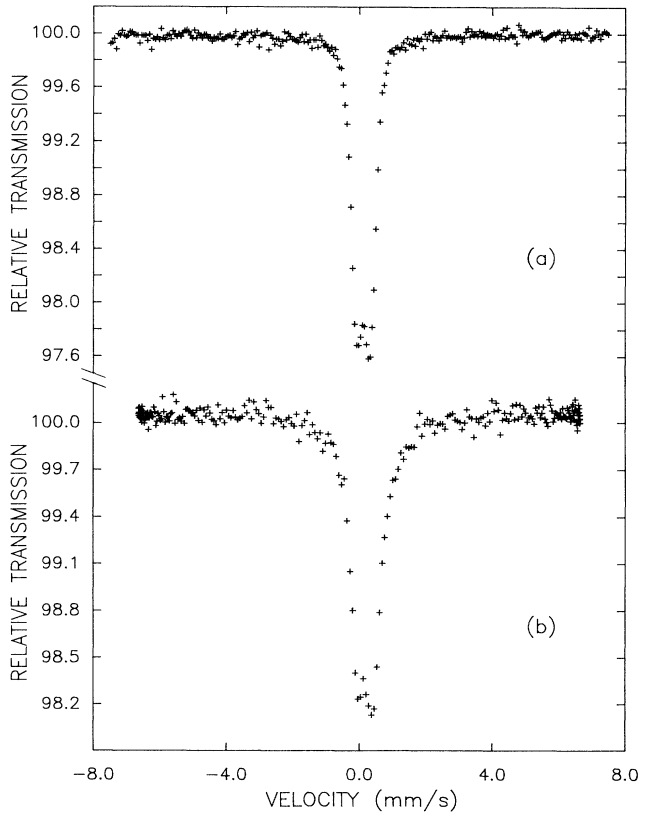

FIG. 7. Room-temperature ^{57}Fe Mössbauer spectra of icosahedral (a) $Al_{52.5}Ge_{22.5}Mn_{24.85}Fe_{0.15}$ and (b) $Al_{40}Cu_{9.94}Fe_{0.06}Ge_{25}Mn_{25}$. The velocity scale is relative to the ^{57}Co(Rh) source.

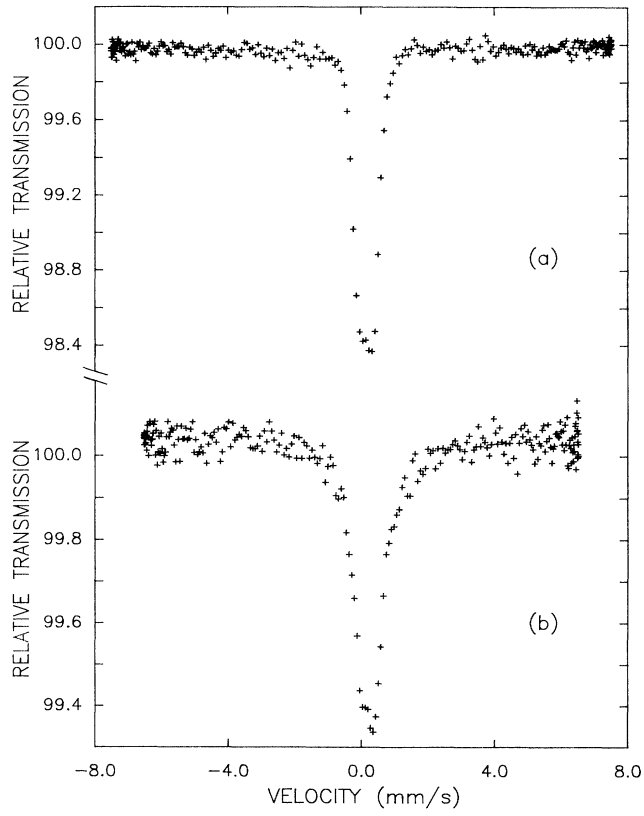

FIG. 8. 4.2-K ^{57}Fe Mössbauer spectra of icosahedral (a) $Al_{52.5}Ge_{22.5}Mn_{24.85}Fe_{0.15}$ and (b) $Al_{40}Cu_{9.94}Fe_{0.06}Ge_{25}Mn_{25}$. The velocity scale is relative to the ^{57}Co(Rh) source.

$\Gamma_{nat}=0.194$ mm/s reflects the presence of a distribution of quadrupole splittings, Δ, as we discussed in detail elsewhere.[9] In order to take this distribution into account, the spectra were fitted to a shell model,[9] for which the distribution function $P(\Delta)=\Delta^{n-1}/\sigma^n\exp(-\Delta^2/2\sigma^2)$ and by assuming a quadratic correlation between the isomer shift δ and Δ ($\delta=\delta_0+a\Delta+b\Delta^2$). The details of the fitting procedure and its justification were described earlier.[9] Attempts to include in the fits a doublet subspectrum due to the AlGeMn(Fe) second phase failed. This indicates that its content is below the resolution of ^{57}Fe Mössbauer spectroscopy. The parameters from the fit of the $Al_{52.5}Ge_{22.5}Mn_{24.85}Fe_{0.15}$ spectrum [solid line in Fig. 9(a)], which are $n=2.053(61)$, $\sigma=0.329(7)$ mm/s, $\Gamma=0.239(6)$ mm/s, $\delta_0=0.145$ mm/s, $a=-0.113(15)$ (mm/s)$^{-1}$, and $b=0.114(17)$ (mm/s)$^{-2}$, gave the average values $\bar{\Delta}=0.418(5)$ mm/s and $\bar{\delta}=0.122(2)$ mm/s. The parameters from the fit of the $Al_{40}Cu_{9.94}Fe_{0.06}Ge_{25}Mn_{25}$ spectrum [solid lline in Fig. 9(b)], which are $n=1.565(57)$, $\sigma=0.396(12)$ mm/s, $\Gamma=0.211(11)$ mm/s, $\delta_0=0.178(4)$ mm/s, $a=-0.095(19)$ (mm/s)$^{-1}$, and $b=0.087(22)$ (mm/s)$^{-2}$, gave $\bar{\Delta}=0.426(5)$ mm/s and $\bar{\delta}=0.159(2)$ mm/s. The fits describe well the experimental spectra [Figs. 9(a) and 9(b)], and the Γ values obtained from the fits are, as expected,[9] only slightly broader than Γ_{nat}. The distribution function $P(\Delta)$ is slightly broader for $Al_{40}Cu_{9.94}Fe_{0.06}Ge_{25}Mn_{25}$ than for $Al_{52.5}Ge_{22.5}Mn_{24.85}Fe_{0.15}$ [Fig. 9(c)]. However, the values of $\bar{\Delta}$ are practically the same in these two alloys. The presence of a distribution of quadrupole splittings in ^{57}Fe Mössbauer spectra of icosahedral alloys observed here and in other icosahedral systems[1,9] is evidence for a continuous distribution of transition-metal sites in these alloys. This reflects the intrinsic disorder present in icosahedral alloys.[1,9,30]

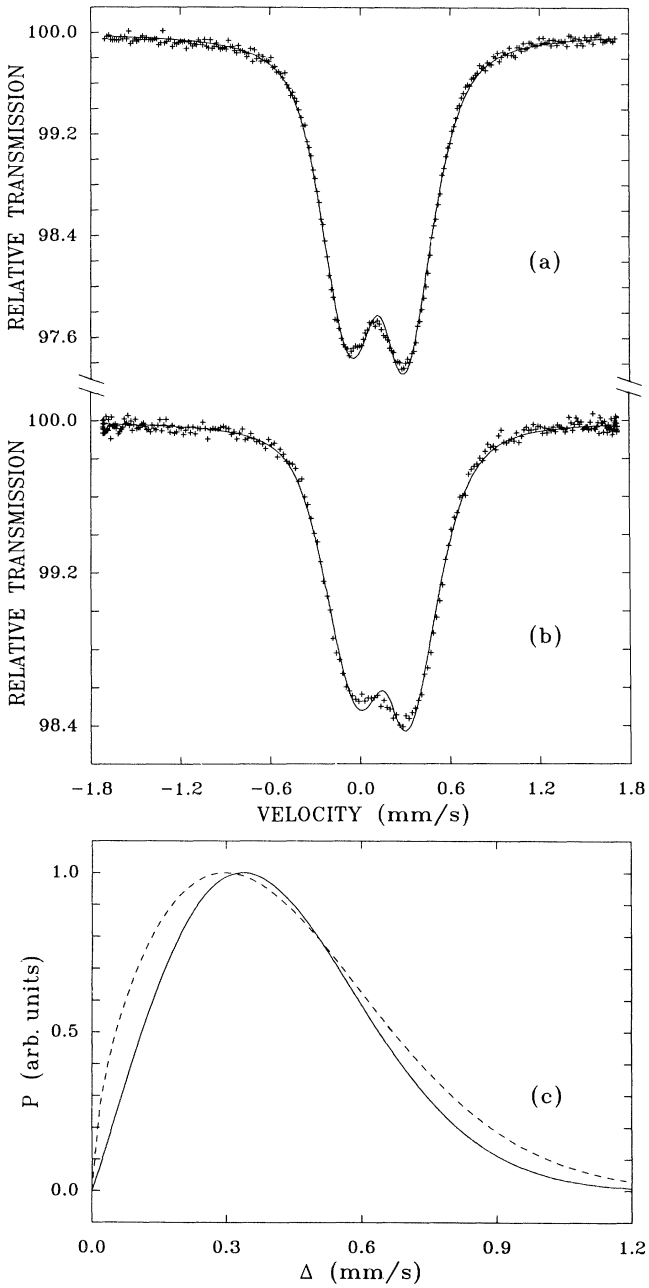

FIG. 9. Room-temperature ^{57}Fe Mössbauer spectra of icosahedral (a) $Al_{52.5}Ge_{22.5}Mn_{24.85}Fe_{0.15}$ and (b) $Al_{40}Cu_{9.94}Fe_{0.06}Ge_{25}Mn_{25}$ fitted (solid line) to a shell model. The velocity scale is relative to the ^{57}Co(Rh) source. The resulting distribution function $P(\Delta)$ corresponding to fits in (a) (solid line) and (b) (dashed line).

Fits of the experimental spectra in Figs. 9(a) and 9(b) to a two-site model[31] gave unphysically broad component lines. This is in accordance with our previous[1,9] and literature[30] studies, which showed that both zero-field and in-field Mössbauer spectra are at variance with such a model. In spite of this clear evidence,[1,9,30] this model is still being used to fit Mössbauer spectra of icosahedral alloys, which leads not only to unphysically broad component lines, but also to values of Γ smaller than Γ_{nat} (see Table 1 in Ref. 32), which is unphysical.

The dominant feature of the 4.2-K ^{57}Fe Mössbauer spectrum of the $Al_{52.5}Ge_{22.5}Mn_{24.85}Fe_{0.15}$ alloy [Fig. 10(a)] is a doublet feature significantly broadened, especially at the wings, as compared to the room-temperature spectrum of this alloy [Fig. 9(a)]. The doublet structure is less visible and the broadening is even larger in the 4.2-K spectrum of the $Al_{40}Cu_{9.94}Fe_{0.06}Ge_{25}Mn_{25}$ alloy [Fig. 10(b)] as compared to the room-temperature spectrum of this alloy [Fig. 9(b)]. This broadening is the evidence for the nonzero value of the hyperfine magnetic field H_{hf} in both alloys. For $H_{hf}=0$ the experimental spectra in Fig. 10 would have had the same structure as the spectra in Fig. 9, with practically negligible line broadening due to increase of the Debye-Waller factor at 4.2 K [compare, for example, the spectrum in Fig. 2(a) from Ref. 9 with the spectrum in Fig. 2 from Ref. 1]. Thus the spectra in Fig. 10 exhibit mixed hyperfine magnetic interactions of comparable strength; i.e., they result from the presence of both an electric quadrupole interaction $E2$ (as is obvious from Fig. 9) and of a magnetic dipole interaction $M1$. For the majority of magnetic systems, $M1$ is much larger than $E2$, and therefore Mössbauer spectra can be fitted using first-order perturbation theory (FOPT), in which $E2$ is treated as a pertur-

bation of the dominant $M1$ (Ref. 29). However, for magnetic systems in which $E2$ and $M1$ are comparable in strength, as is the case here, FOPT is invalid, and the exact Hamiltonian method must be used.[33]

^{57}Fe Mössbauer spectra of $Al_{40}Cu_{10-x}Fe_xGe_{25}Mn_{25}$ icosahedral alloys with $x=3$, 6, and 10 measured at room temperature[5,6] and at 110 K (for composition $x=3$, Ref. 5) were fitted using the FOPT to a six-line Zeeman pattern. Such fits are erroneous for two reasons. First, as is clearly shown in Fig. 9(b), the room-temperature Mössbauer spectrum for the composition $x=0.06$ is due to $E2$ only. Substituting more Fe for Cu merely introduces more disorder, which is reflected in a slight line broadening of the doublet pattern.[18] Furthermore, $E2$ is present in all Al-based icosahedral alloys studied so far. Thus fitting room-temperature Mössbauer spectra which are due entirely to $E2$ with a Zeeman pattern[5,6] is unphysical. It was assumed[5,6] that since T_C of $Al_{40}Cu_{10}Ge_{25}Mn_{25}$ is 467 K,[3] ^{57}Fe Mössbauer spectra at room temperature must be due to $M1$. But as was indicated above, the high value of the reported T_C is due to the presence of a AlGeMn second phase, and the real value of T_C of $Al_{40}Cu_{10}Ge_{25}Mn_{25}$, as is argued below, must be much lower. Second, the spectrum of $Al_{40}Cu_7Fe_3Ge_{25}Mn_{25}$ at 110 K [Fig. 2(a) in Ref. 5] exhibits minute broadening as compared to the room-temperature spectrum [Fig. 2(b) in Ref. 5], which seems to indicate the presence of not only $E2$, but also $M1$, with strengths of the same order of magnitude. Consequently, one cannot fit such a spectrum to a Zeeman pattern using the FOPT. Furthermore, it was claimed[5,6] that the quadrupole splitting obtained from such fits is essentially zero. This is not surprising since in the FOPT method the shift of component lines of a Zeeman pattern due to $E2$ is proportional to K, with $K=(3\cos^2\theta-1+\eta\sin^2\theta\cos2\phi)/2$, where η is the asymmetry parameter, and θ and ϕ are the polar angles of H_{hf} with respect to the principal axis system of the electric-field-gradient (EFG) tensor.[34] For systems with disorder, such as icosahedral alloys, θ and ϕ are randomly distributed, and consequently the average of K is zero.[34] Thus there will be no shift of Zeeman lines due to $E2$ in spite of the nonzero $E2$. The above arguments also hold for fits[5,6] of Mössbauer spectra of the $Al_{40}Cu_{10-x}Fe_xGe_{25}Mn_{25}$ series using the method of Le-Caer and Dubois.[35] The distributions of H_{hf} obtained from such fits are meaningless. We conclude that the previous analysis[5,6] of the ^{57}Fe Mössbauer spectra of $Al_{40}Cu_{10-x}Fe_xGe_{25}Mn_{25}$ is incorrect, and consequently the conclusions based on it and reported in the literature[17] as established facts are invalid.

Since 4.2-K experimental Mössbauer spectra of $Al_{52.5}Ge_{22.5}Mn_{24.85}Fe_{0.15}$ and $Al_{40}Cu_{9.94}Fe_{0.06}Ge_{25}Mn_{25}$ icosahedral alloys show mixed hyperfine magnetic dipole and electric quadrupole interactions of comparable magnitude, they have here been treated using the exact Hamiltonian. Because of the presence of disorder, which is an inherent property of icosahedral alloys, it was assumed that there is no correlation between the EFG principal axes and the direction of H_{hf}. We employed the algoirthm given by Blaes, Fischer, and Gonser,[36] which is suitable for such a case.

The fitting routine provides δ, H_{hf}, the quadrupole couling constant $QS=eQV_{zz}/2$ (e is the electron charge, Q is the quadrupole moment of the ^{57}Fe nucleus, and V_{zz} is the principal component of the EFG tensor), η, and α (the angle between the gamma ray and the direction of H_{hf}). Since in reality all the above parameters exhibit some distribution, their values obtained from such a one-site fit can be regarded as the average values, just as one can treat a quadrupole splitting Δ obtained from an asymmetric doublet fit to a spectrum exhibiting a distribution of Δ values.[9] Because of the smallness of the magnetic dipole interaction manifested in the broadening of the 4.2-K Mössbauer spectra, it is impossible to fit such spectra using a distribution of the various hyperfine parameters. However, this distribution has been taken indirectly into account by fixing the value of Γ in the fits to the weighted average of the linewidths of the two component lines obtained from the fits of the room-temperature spectra in Fig. 9 with an asymmetric doublet. These values are 0.398 mm/s for $Al_{52.5}Ge_{22.5}Mn_{24.85}Fe_{0.15}$ 0.416 mm/s for $Al_{40}Cu_{9.94}Fe_{0.06}Ge_{25}Mn_{25}$. It should be emphasized that the fitted parameters do not differ too much for other choices of Γ values. Attempts to improve the fits by including an additional spectrum due to AlGeMn(Fe) impurity (Fig. 6) resulted in zero intensity for such a spectrum. It shows that the amount of this impurity is below the resolution of the ^{57}Fe ME technique.

The fits obtained using the above fitting procedure are presented in Fig. 10. The parameters obtained from the fit for $Al_{52.5}Ge_{22.5}Mn_{24.85}Fe_{0.15}$ are $\delta=0.205(1)$ mm/s, $H_{hf}=8.8(2)$ kOe, $QS=-0.452(2)$ mm/s, $\eta=0.1(1)$, and $\alpha=90(20)°$. The corresponding parameters for $Al_{40}Cu_{9.94}Fe_{0.06}Ge_{25}Mn_{25}$ are 0.234(4) mm/s, 11.8(5) kOe, $-0.438(6)$ mm/s, $\eta=0.1(1)$, and $\alpha=90(25)°$. The fits are very sensitive to the values of δ, H_{hf}, and QS, but only marginally sensitive to η and α. Therefore, the values of η and α are only estimations.

The temperature changes of δ between room temperature (295 K) and 4.2 K are -2.85×10^{-4} and -2.58×10^{-4} (mm/s) K for $Al_{52.5}Ge_{22.5}Mn_{24.85}Fe_{0.15}$ and $Al_{40}Cu_{9.94}Fe_{0.06}Ge_{25}Mn_{25}$, respectively. The decrease of δ with temperature is due to the second-order Doppler effect.[29] The similar values of QS for both alloys are consistent with the similar values of $\bar{\Delta}$ obtained from the fits of room-temperature spectra [Figs. 9(a) and 9(b)] with a shell model. The predominant negative sign of QS is consistent with the same predominant sign of QS obtained from in-field ^{57}Fe Mössbauer spectra of paramagnetic Al-based alloys.[30] It indicates that the local environment around Fe atoms in these alloys is similar to the environment in other Al-based alloys.[30] Because of the lack of structural studies of the local environment of transition-metal atoms in the studied alloys, it is not possible at present to associate QS values with a particular local structure model.

There are several contributions to H_{hf}.[29] A quantitative analysis of these contributions is very complex.

However, to the first approximation, the dominant contributions in metallic systems are the contribution due to the core electrons, H_{hf}^{c}, and the contribution due to the conduction electrons, H_{hf}^{con}. On the basis of experimental data for various Fe-based alloys, it was suggested[37] that $H_{hf}=H_{hf}^{c}+H_{hf}^{con}=a\mu_{Fe}+b\bar{\mu}$, where μ_{Fe} is the magnetic moment of Fe atoms in a given alloy, $\bar{\mu}$ is the average magnetic moment per magnetic atom in the alloy, and a and b are proportionality constants. There is a firm theoretical basis for the proportionality between H_{hf}^{c} and μ_{Fe}.[38–40] However, there is no such theoretical basis for the assumption that $H_{hf}^{con}=b\bar{\mu}$.[39,40] In fact, H_{hf}^{con} may depend in a complex way upon the electronic structure parameters of the alloy. Nevertheless, H_{hf}^{con} in most cases scales with H_{hf}^{c} and usually $H_{hf}^{c}\gg H_{hf}^{con}$,[38,39] which explains the generally good agreement between μ_{Fe} values derived from ^{57}Fe ME experiments and the values derived, for example, from neutron scattering. Using $a=142$ kOe/μ_B, which is a typical value found for many alloys,[40,41] and assuming $b=0$, one can estimate from the measured values of H_{hf} that μ_{Fe} at 4.2 K is $0.06\mu_B$ and $0.08\mu_B$ for $Al_{52.5}Ge_{22.5}Mn_{24.85}Fe_{0.15}$ and $Al_{40}Cu_{9.94}Fe_{0.06}Ge_{25}Mn_{25}$, respectively. Such small values of μ_{Fe} indicate that Fe atoms in the studied alloys are slightly above the borderline between possessing and not possessing a magnetic moment. Since Fe atoms in the alloys are at the impurity concentration level, the nonzero values of μ_{Fe} suggest nonzero values of μ_{Mn}. Even if one assumes that all measured H_{hf} are due to the conduction electrons (which means that $\mu_{Fe}=0$), which is a much less probable situation, the presence of H_{hf} implies nonzero value of μ_{Mn} since conduction-electron polarization can be achieved only when $\mu_{Mn}\neq 0$. The values of μ_{Mn} are expected to be very small: about a few hundredths of μ_B for $Al_{52.5}Ge_{22.5}Mn_{24.85}Fe_{0.15}$ and about $0.1\mu_B$ for $Al_{40}Cu_{9.94}Fe_{0.06}Ge_{25}Mn_{25}$ based on the estimates of saturation magnetizations of these alloys and assuming that the measured values of M for the samples with the least amount of second phases are due solely to the icosahedral phase. The effective magnetic moment per Mn atom, p_{eff}, derived from the temperature dependence of susceptibility data for many Al-based paramagnetic icosahedral alloys is of the order of $1\mu_B$. It seems not unreasonable to assume that p_{eff} in the studied alloys is of the same order of magnitude. Combining this assumption with the fact of the very small value of the saturation magnetic moment suggests, on the basis of the Rhodes-Wohlfarth plot,[42] a very small T_C. The analysis presented above indicates that at 4.2 K both Fe and Mn atoms in the studied alloys carry a very small magnetic moment. It seems also that T_C of these icosahedral alloys is not much above 4.2 K, and that at 4.2 K they are only slightly above the borderline between being and not being magnetic.

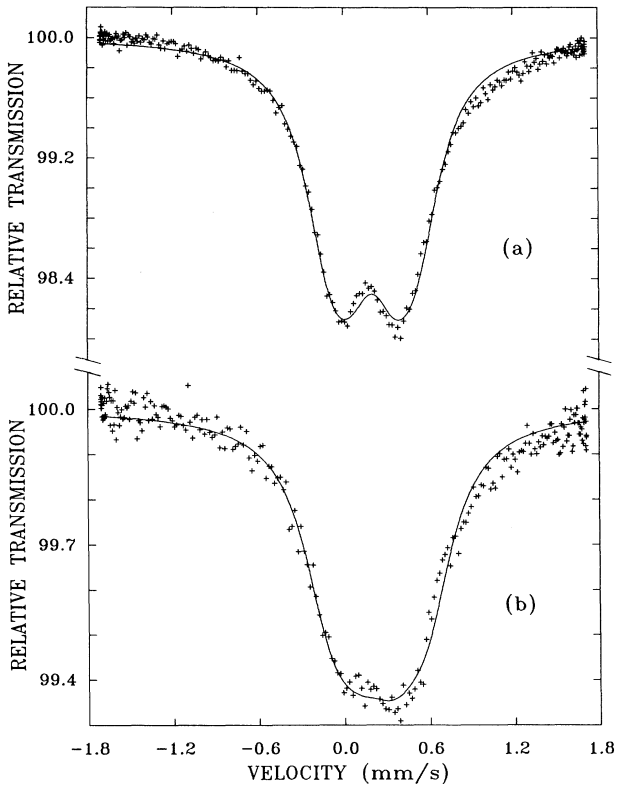

FIG. 10. 4.2-K ^{57}Fe Mössbauer spectra of icosahedral (a) $Al_{52.5}Ge_{22.5}Mn_{24.85}Fe_{0.15}$ and (b) $Al_{40}Cu_{9.94}Fe_{0.06}Ge_{25}Mn_{25}$. The velocity scale is relative to the ^{57}Co(Rh) source. The fits (solid lines) are explained in the text.

There is another, equally valid possible interpretation of the 4.2-K Mössbauer spectra of $Al_{52.5}Ge_{22.5}Mn_{24.85}Fe_{0.15}$ and $Al_{40}Cu_{9.94}Fe_{0.06}Ge_{25}Mn_{25}$ icosahedral alloys, which complements the above interpretation. The fits shown in Fig. 10 are not satisfactory at the wings and in the central part of the spectra. A further improvement of the fits was possible by using two subspectra. In the first subspectrum, $H_{hf}(1)=0$ was set, which corresponds to the assumption that at 4.2 K some of Fe atoms are nonmagnetic, and the other parameters, except δ_1 and the subspectrum relative area A_1, were set to the values obtained from an asymmetric doublet fit of the room-temperature spectra (this is justified since the temperature dependence of the quadrupole splitting is negligibly small[1]). All parameters of the second subspectrum, i.e., δ_2, $H_{hf}(2)$, QS_2, η_2, α_2, and A_2, were fitted. Similarly to the fits in Fig. 10, the value of Γ_2 was fixed. The fits shown in Fig. 11 account well for the features at the wings and in the central part of the experimental spectra. Attempts to include a third subspectrum due to the AlGeMn(Fe) second phase with parameters derived from Fig. 6 did not produce a better fit. The fraction of this subspectrum was below 1% and was not statistically meaningful. It does not mean that this second phase is not present in the studied samples. It only shows that its content is below the resolution of ^{57}Fe Mössbauer spectroscopy. The parameters obtained from the fit for $Al_{52.5}Ge_{22.5}Mn_{24.85}Fe_{0.15}$ [Fig. 11(a)] are $\delta_1=0.187(1)$ mm/s, $A_1=0.69$, $\delta_2=0.239(1)$ mm/s, $H_{hf}(2)=32.2(1)$ kOe, $QS_2=0.000(2)$ mm/s, $\eta_2=0.0(1)$, $\alpha_2=90(20)°$, and $A_2=0.31$. The corresponding parameters for

$Al_{40}Cu_{9.94}Fe_{0.06}Ge_{25}Mn_{25}$ [Fig. 11(b)] are 0.195(5) mm/s, 0.54, 0.289(10) mm/s, 28.7(7) kOe, −0.355(25) mm/s, 0.0(1), 90(25)°, and 0.46. Freeing $H_{hf}(1)$ in the fit resulted in a practically zero value, which justifies the assumption made. The fits were practically insensitive to the values of η_2 and α_2. Therefore, the values of these parameters should be treated as only estimations. The values of μ_{Fe} estimated from the values of $H_{hf}(2)$, using the procedure described earlier, are $0.23\mu_B$ for $Al_{52.5}Ge_{22.5}Mn_{24.85}Fe_{0.15}$ and $0.20\mu_B$ for $Al_{40}Cu_{9.94}Fe_{0.06}Ge_{25}Mn_{25}$.

There are, in principle, two possible explanations for the results of two-component fits. In the first explanation one could interpret the nonmagnetic subspectrum as evidence that the studied icosahedral alloys are not magnetically ordered (provided that $\mu_{Fe}=0$ implies that $\mu_{Mn}=0$), whereas the magnetic subspectrum would be interpreted as being due to 31% of Fe atoms for $Al_{52.5}Ge_{22.5}Mn_{24.85}Fe_{0.15}$ and 46% of Fe atoms for $Al_{40}Cu_{9.94}Fe_{0.06}Ge_{25}Mn_{25}$ substituting respectively for Mn and Cu atoms not of icosahdral alloys, but of magnetic crystalline second phases. An argument against such an explanation is as follows. As was shown with XRD analysis, the main second phase present in the studied alloys is AlGeMn. Because the 4.2-K ^{47}Fe Mössbauer spectrum of this phase (in which Fe was substituted in the impurity concentration for Mn) is a quadrupole doublet (Fig. 6), its presence cannot thus be responsible for the magnetic subspectrum. Fe atoms in other unidentified phases could, in principle, contribute to this spectrum. However, the large fraction of the magnetic subspectrum is incompatible with XRD results, which indicate the presence of a very small fraction of second phases *other than* AlGeMn (Figs. 2 and 3). Such an explanation seems therefore to be unlikely.

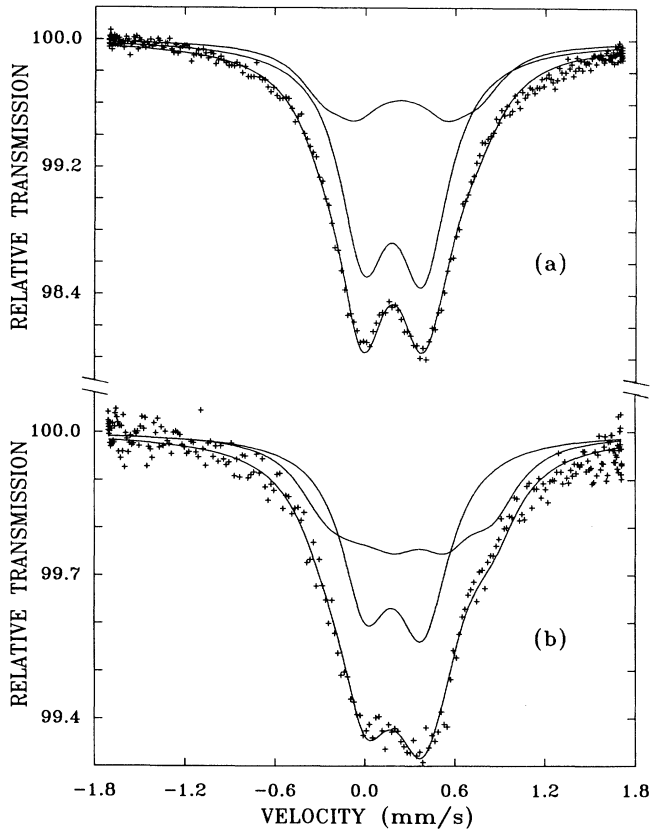

FIG. 11. 4.2-k ^{57}Fe Mössbauer spectra of icosahedral (a) $Al_{52.5}Ge_{22.5}Mn_{24.85}Fe_{0.15}$ and (b) $Al_{40}Cu_{9.94}Fe_{0.06}Ge_{25}Mn_{25}$. The velocity scale is relative to the ^{57}Co(Rh) source. The fits (solid lines) with two subspectra, which are also shown (solid lines), are explained in the text.

The second possible explanation is based on the hypothesis of two classes of transition-metal sites in Al-based icosahedral alloys, which was reviewed in Ref. 1. Briefly, there is a strong experimental evidence[1] which suggests that there are two classes (or two distributions) of transition-metal sites in Al-based icosahedral alloys: larger sites which allow moment formation and smaller sites which are nonmagnetic. In the alloys studied so far, Fe atoms seem to substitute only the latter, and consequently they bear no magnetic moment. However, in a recent study Eibschütz *et al.*[43] confirmed, using susceptibility measurements, an earlier conclusion based on extended x-ray absorption fine structure studies[44] of Al-Mn-Fe and Al-Mn-Fe-Si icosahedral alloys that *small amounts* of Fe atoms substitute randomly for Mn atoms: i.e., they enter both magnetic and nonmagnetic classes of Mn sites. As has been often stressed in the literature,[1,43,45] the two classes of sites should not be confused with the existence of two approximately well-defined crystallographic sites. The two classes of sites imply the presence of two distributions of sites. If one assumes that in the studied alloys the local environment of transition-metal atoms is similar to the environment in Al-Mn-Fe and Al-Mn-Fe-Si icosahedral alloys (a negative sign of QS, as discussed earlier, gives credence to such an assumption), then one can also expect the presence of two classes of transition-metal sites in these alloys. Because of the low concentration of Fe atoms in the studied alloys, these atoms would then enter approximately randomly[43,44] these two classes of sites. One would thus expect to observe a nonmagnetic subspectrum due to the Fe atoms entering the nonmagnetic class of sites and a magnetic subspectrum due to the Fe atoms entering the magnetic class of sites, which is consistent with our observations (Fig. 11).

IV. SUMMARY

A critical review of magnetically ordered icosahedral alloys has been presented. It has been argued on the basis of literature data that ferromagnetism in Si-rich Al-Mn-Si alloys is an impurity effect rather than an intrinsic property. It has been shown with x-ray diffraction and magnetization measurements that an AlGeMn ferromagnet is the major second phases present in Al-Ge-Mn and Al-Cu-Ge-Mn icosahedral samples and is partially responsible for their magnetism. It has been shown that this ferromagnet is the main crystallization product of Al-Ge-Mn and Al-Cu-Ge-Mn icosahedral alloys. Room-temperature ^{57}Fe Mössbauer spectra of

$Al_{52.5}Ge_{22.5}Mn_{24.85}Fe_{0.15}$ and $Al_{40}Cu_{9.94}Fe_{0.06}Ge_{25}Mn_{25}$ icosahedral alloys prove, contrary to previous erroneous analysis of Mössbauer spectra, that Fe atoms do not carry a magnetic moment. Their analysis shows that Fe atoms are distributed among a multiplicity of sites, which reflects intrinsic disorder present in icosahedral alloys. Analysis of 4.2-K Mössbauer spectra of these alloys shows that Fe atoms bear a small magnetic moment. We show that this suggests that the magnetic moment of Mn as well as T_C of Al-Ge-Mn and Al-Cu-Ge-Mn icosahedral alloys should be very small. It has been shown that, in agreement with other experimental studies, 4.2-K Mössbauer spectra indicate the existence of two classes of transition-metal sites: a nonmagnetic class of sites, in which Fe atoms bear no magnetic moment, and a magnetic class of sites, in which Fe atoms possess a magnetic moment. Al-Ge-Mn and Al-Cu-Ge-Mn icosahedral alloys seem to be slightly above the borderline between being nonmagnetic and magnetic. Finally, it has been observed that annealing rapidly quenched samples of Al-Ge-Mn and Al-Cu-Ge-Mn icosahedral alloys leads to a significant increase of the coercive force and saturation magnetization. This suggests that these materials have the potential of being used as permanent magnets.

ACKNOWLEDGMENTS

This work was supported by the Natural Science and Engineering Research Council of Canada. The technical assistance provided by B. Fullerton and G. Viau is appreciated. We thank R. A. Brand for making his computer program available to us.

*Permanent address: Department of Physics, University of Ottawa, 34 George Glinski, Ottawa, Ontario, Canada K1N 6N5.

[1]Z. M. Stadnik, G. Stroink, H. Ma, and G. Williams, Phys. Rev. B **39**, 9797 (1989), and references therein.

[2]J. G. Zhao, L. Y. Yang, Q. Fu, and H. Q. Guo, Chin. Phys. Lett. **5**, 405 (1988).

[3]A. P. Tsai, A. Inoue, T. Masumoto, and N. Kataoka, Jpn. J. Appl. Phys. **27**, L2252 (1988).

[4]R. A. Dunlap, M. E. McHenry, V. Srinivas, D. Bahadur, and R. C. O'Handley, Phys. Rev. B **39**, 4808 (1989).

[5]R. A. Dunlap and V. Srinivas, Phys. Rev. B **40**, 704 (1989).

[6]V. Srinivas, R. A. Dunlap, D. J. Lloyd, and S. Jha, Hyperfine Interact. (to be published).

[7]V. Srinivas, R. A. Dunlap, M. E. McHenry, and R. C. O'Handley, J. Appl. Phys. **67**, 5879 (1990).

[8]Z. M. Stadnik and G. Stroink, J. Appl. Phys. **67**, 5891 (1990).

[9]Z. M. Stadnik and G. Stroink, Phys. Rev. B **38**, 10447 (1988), and references therein.

[10]S. Matsuo, T. Ishimasa, H. Nakano, and Y. Fukano, J. Phys. F **18**, L175 (1988).

[11]J. J. Hauser, H. S. Chen, and J. V. Waszczak, Phys. Rev. B **33**, 3577 (1986).

[12]J. J. Hauser, H. S. Chen, G. P. Espinosa, and J. V. Waszczak, Phys. Rev. B **34**, 4674 (1986).

[13]K. Fukamichi, T. Goto, H. Wakabayashi, Y. Bizen, A. Inoue, and T. Masumoto, Sci. Rep. Res. Inst. Tohoku Univ. A **34**, 93 (1988).

[14]S. K. Misra, L. E. Misiak, D. Bahadur, V. Srinivas, and R. A. Dunlap, Phys. Rev. B **40**, 7537 (1989).

[15]The crystalline Si-rich Al-Mn-Si phase with $T_C = 110$ K must have a different structure than the β-Al-Mn-Si alloy [K. Robinson, Acta Crstallogr. **5**, 26 (1952)] since the latter is known to be a paramagnet between 4.2 K and room temperature [R. Bellissent, F. Hippert, P. Monod, and F. Vigneron, Phys. Rev. B **36**, 5540 (1987)].

[16]R. C. O'Handley, R. A. Dunlap, and M. E. McHenry, Philos. Mag. B **61**, 677 (1990).

[17]R. C. O'Handley, R. A. Dunlap, and M. E. McHenry, in *Ferromagnetic Materials,* edited by K. H. J. Buschow (in press).

[18]Z. M. Stadnik and G. Stroink (unpublished).

[19]W. A. J. J. Velge and K. J. De Vos, J. Appl. Phys. **34**, 3568 (1963); K. Shibata, T. Shinohara, and H. Watanabe, J. Phys. Soc. Jpn. **33**, 1328 (1972); K. Shibata, H. Watanabe, H. Yamauchi, and T. Shinohara, *ibid.* **35**, 448 (1973).

[20]Certificate of Calibration, Iron Foil Mössbauer Standard, Natl. Bur. Stand. (U.S.) Circ. No. 1541, edited by J. P. Cali (U.S. GPO, Washington, D.C., 1971).

[21]J. H. Wernick, S. E. Haszko, and W. J. Romanow, J. Appl. Phys. **32**, 2495 (1961); N. S. Satya Murthy, R. J. Begum, C. S. Somanathan, and M. R. L. N. Murthy, *ibid.* **40**, 1870 (1969); G. B. Street, J. Solid State Chem. **7**, 316 (1973).

[22]N. Yamada, J. Phys. Soc. Jpn. **59**, 273 (1990), and references therein.

[23]P. A. Bancel, P. A. Heiney, P. W. Stephens, A. I. Goldman, and P. M. Horn, Phys. Rev. Lett. **54**, 2422 (1985).

[24]V. Elser and Ch. L. Henley, Phys. Rev. Lett. **55**, 2883 (1985).

[25]V. Elser, Phys. Rev. B **32**, 4892 (1985).

[26]M. Laridjani, M. Bigare, and A. Guinier, Mem. Sci. Rev. Metall. **67**, 675 (1970).

[27]T. Shinohara, S. Kurosawa, and H. Onodera, J. Phys. Soc. Jpn. **50**, 1877 (1981).

[28]T. Kamimura, H. Ido, and K. Shirakawa, J. Appl. Phys. **57**, 3255 (1985).

[29]N. N. Greenwood and T. C. Gibb, *Mössbauer Spectroscopy* (Chapman and Hall, London, 1971).

[30]G. LeCaër, R. A. Brand, and J. M. Dubois, Philos. Mag. Lett. **56**, 143 (1987); G. LeCaër, R. A. Brand, and J. M. Dubois, Hyperfine Interact. **42**, 943 (1988); R. A. Brand, G. LeCaër, and J. M. Dubois, J. Phys. Condens. Matter **2**, 6413 (1990).

[31]L. J. Swartzendruber, S. Shechtman, L. Bendersky, and J. W. Cahn, Phys. Rev. B **32**, 1383 (1985); R. A. Dunlap, D. W. Lawther, and D. J. Lloyd, *ibid.* **38**, 3649 (1988).

[32]V. Srinivas, R. A. Dunlap, D. Bahadur, and E. Dunlap, Philos. Mag. B **61**, 177 (1990).

[33]R. A. Brand, Nucl. Instrum. Methods Phys. Res. B **28** 398 (1987), and references therein.

[34]G. LeCaër, J. M. Dubois, H. Fisher, U. Gonser, and H. G. Wagner, Nucl. Instrum. Methods Phys. Res. B **2**, 201 (1985).

[35]G. LeCaër and J. M. Dubois, J. Phys. E **12**, 1083 (1979).

[36]N. Blaes, H. Fischer, and U. Gonser, Nucl. Instrum. Methods Phys. Res. B **9**, 201 (1985).

[37]C. E. Johnson, M. S. Ridout, T. E. Cranshaw, and P. E. Madsen, Phys. Rev. Lett. **6**, 450 (1961); C. E. Johnson, M. S. Ridout, and T. E. Cranshaw, in *The Mössbauer Effect,* edited by D. M. J. Compton and A. H. Schoen (Wiley, New York,

1961), p. 141; C. E. Johnson, M. S. Ridout, and T. E. Cranshaw, Proc. Phys. Soc. London **81**, 1079 (1963).
[38]A. J. Freeman and R. E. Watson, in *Magnetism,* edited by G. T. Rado and H. Suhl (Academic, New York, 1965), Vol. IIA, p. 167.
[39]H. Ebert, H. Winter, B. L. Gyorffy, D. D. Johnson, and F. J. Pinski, J. Phys. F **18**, 719 (1988).
[40]O. Erikson and A. Svane, J. Phys. Condens. Matter **1**, 1589 (1989).
[41]Z. M. Stadnik and G. Stroink, Hyperfine Interact. **47**, 275 (1989).
[42]P. Rhodes and E. P. Wohlfarth, Proc. R. Soc. London **273**, 247 (1963); E. P. Wohlfarth, J. Magn. Magn. Mater. **7**, 113 (1978).
[43]M. Eibschütz, M. E. Lines, H. S. Chen, and J. V. Waszczak, Phys. Rev. B **41**, 4606 (1990).
[44]Y. Ma and E. A. Stern, Phys. Rev. B **35**, 2678 (1987).
[45]W. W. Warren, H.-S. Chen, and G. P. Espinosa, Phys. Rev. B **34**, 4902 (1986).